Geophysical Research Letters

RESEARCH LETTER
10.1029/2018GL081731

Long-Term Measurements Show Little Evidence for Large Increases in Total U.S. Methane Emissions Over the Past Decade

Xin Lan[1,2], Pieter Tans[2], Colm Sweeney[2], Arlyn Andrews[2], Edward Dlugokencky[2], Stefan Schwietzke[1,2], Jonathan Kofler[1,2], Kathryn McKain[1,2], Kirk Thoning[2], Molly Crotwell[1,2], Stephen Montzka[2], Benjamin R. Miller[1,2], and Sébastien C. Biraud[3]

[1]Cooperative Institute for Research in Environmental Sciences, University of Colorado Boulder, Boulder, CO, USA, [2]National Oceanic and Atmospheric Administration, Earth System Research Laboratory, Boulder, CO, USA, [3]Lawrence Berkeley National Laboratory, Berkeley, CA, USA

Key Points:
- Long-term measurements show no large increases in U.S. methane emissions in the past decade
- The estimated increase in U.S. oil and natural gas CH_4 emissions is an order of magnitude lower than some previous studies
- The increasing trend in C_2H_6/CH_4 emission ratios has resulted in major overestimation of an oil and gas emissions trend in some previous studies

Supporting Information:
- Supporting Information S1

Correspondence to:
X. Lan,
xin.lan@noaa.gov

Citation:
Lan, X., Tans, P., Sweeney, C., Andrews, A., Dlugokencky, E., Schwietzke, S., et al. (2019). Long-term measurements show little evidence for large increases in total U.S. methane emissions over the past decade. *Geophysical Research Letters*, *46*, 4991–4999. https://doi.org/10.1029/2018GL081731

Received 17 DEC 2018
Accepted 18 APR 2019
Accepted article online 25 APR 2019
Published online 15 MAY 2019

Abstract Recent studies show conflicting estimates of trends in methane (CH_4) emissions from oil and natural gas (ONG) operations in the United States. We analyze atmospheric CH_4 measurements from 20 North American sites in the National Oceanic and Atmospheric Administration Global Greenhouse Gas Reference Network and determined trends for 2006–2015. Using CH_4 vertical gradients as an indicator of regional surface emissions, we find no significant increase in emissions at most sites and modest increases at three sites heavily influenced by ONG activities. Our estimated increases in North American ONG CH_4 emissions (on average approximately 3.4 ± 1.4 %/year for 2006–2015, ±σ) are much smaller than estimates from some previous studies and below our detection threshold for total emissions increases at the east coast sites that are sensitive to U.S. outflows. We also find an increasing trend in ethane/methane emission ratios, which has resulted in major overestimation of oil and gas emissions trends in some previous studies.

Plain Language Summary In the past decade, natural gas production in the United States has increased by ~46%. Methane emissions associated with oil and natural gas productions have raised concerns since methane is a potent greenhouse gas with the second largest influence on global warming. Recent studies show conflicting results regarding whether methane emissions from oil and gas operations have been increased in the United States. Based on long-term and well-calibrated measurements, we find that (i) there is no large increase of total methane emissions in the United States in the past decade; (ii) there is a modest increase in oil and gas methane emissions, but this increase is much lower than some previous studies suggest; and (iii) the assumption of a time-constant relationship between methane and ethane emissions has resulted in major overestimation of an oil and gas emissions trend in some previous studies.

1. Introduction

Atmospheric CH_4 is a well-mixed greenhouse gas with the second largest increase in radiative forcing after carbon dioxide (Butler & Montzka, 2017). It can be released from natural (e.g., wetlands, wild animals, and termites) and anthropogenic sources (e.g., oil and natural gas [ONG] operations, landfills, and agriculture; United States Environmental Protection Agency [EPA], 2017, Saunois et al., 2016). The global atmospheric CH_4 abundance was nearly stable from 1999 through 2006 (Bousquet et al., 2006; Dlugokencky et al., 2003; Dlugokencky et al., 2009), but since then has significantly increased (Dlugokencky, 2018; Nisbet et al., 2016). ONG activities are a large source of atmospheric CH_4 and alkanes such as ethane (C_2H_6), propane (C_3H_8), and others. In the past decade, natural gas production has increased by ~46% in the United States (Figure S1 in the supporting information) due to the development of horizontal drilling and hydraulic-fracturing techniques (U.S. Energy Information Administration, 2016). Several studies conclude that there are substantial increases in ONG CH_4 emissions (Franco et al., 2016; Hausmann et al., 2016; Helmig et al., 2016; Turner et al., 2016), with some (Hausmann et al., 2016; Turner et al., 2016) further suggesting that these have substantially contributed to the global CH_4 increases after 2007. Ethane/methane emission ratios have been used to argue for large increases in ONG CH_4 emissions (Franco et al., 2016; Hausmann et al., 2016; Helmig et al., 2016), since C_2H_6 and CH_4 are coemitted from ONG activities, although Helmig et al. (2016) notes an inconsistency with measurements of CH_4 and its isotopic ratios ($\delta^{13}CH_4$). Measured changes of $\delta^{13}CH_4$ lead to the hypothesis that the global CH_4 rise after 2007 is dominated by biogenic

emissions (Nisbet et al., 2016; Schaefer et al., 2016; Schwietzke et al., 2016). A recent study using an ensemble of global atmospheric inversions constrained by surface observations, with some including satellite retrievals of column-averaged CH_4, finds no statistically significant increase in total North American CH_4 emissions during 2000–2014 (Bruhwiler et al., 2017).

Here we analyze decadal records of CH_4 (2006–2015) and C_3H_8 (2008–2015) from 11 sites where CH_4 vertical profiles are collected from aircraft (Sweeney et al., 2015) and 9 surface sites (including tall towers; Andrews et al., 2014) in the National Oceanic and Atmospheric Administration Global Greenhouse Gas Reference Network (GGGRN; see Figure S2 for site locations). The majority of the sites are designed to capture air masses that are well mixed and thus represent influences of emissions from large areas. According to our footprint and inventory (Maasakkers et al., 2016) analysis in which the sensitivity of observed mole fraction changes to emissions from different sources are estimated (see Figure S3 for footprints), five GGGRN sites are substantially influenced by ONG activities (DND, CAR, SGP, SGP-s, and WKT-s; '-s' following a site code indicates surface site; site codes are given in Table S1 in the supporting information). Thus, these five sites are defined as 'ONG sites' in the following text. The other sites are defined as 'non-ONG sites', although some of them are moderately influenced by ONG emissions. Please refer to Supporting Information (SI) for details of measurement and statistical analysis.

2. Trends in CH_4 and CH_4 Vertical Gradients (ΔCH_4)

Atmospheric methane trends from GGGRN sites demonstrate clear increases after 2006 (e.g., Figures 1a and 1b), similar to the global background CH_4 trend. Excluding the five ONG sites, CH_4 trends in the United States (contiguous 48 states, 'CONUS') are indistinguishable within 1σ uncertainty with an average increase rate of 6.12 ± 0.11 ppb/year (0.33 ± 0.01%/year). This is similar to the trends in the marine boundary layer reference (Dlugokency et al., 2015) of 6.11 ± 0.07 ppb/year for the 25–55°N zonal average and of 6.08 ± 0.04 ppb/year for the global average. For the five ONG sites, a significantly larger trend is measured in CH_4 mole fractions, which is 7.65 ± 0.31 ppb/year (0.40 ± 0.02%/year).

To reveal trends in CONUS CH_4 emissions, we assess CH_4 mole fraction enhancements ('Δ') after removing appropriate background mole fractions, because the background contributes the largest part of CH_4 in ambient air, while enhancements due to regional and local emissions are relatively small. A trend in CH_4 mole fractions (see above) without subtracting the background signals cannot represent the trend in local and regional emissions. We use the midtroposphere (3.5–5.5 km above sea level) as representative of background condition and investigate the trends in ΔCH_4, which are, in this case, also vertical gradients (e.g., Figures 1c and 1d; see SI section 3 for calculation). A lower boundary of 3.5 km ensures free troposphere air, and the upper boundary ensures that the background air masses are not completely detached from the surface since measurements of CH_4 and its trend at high altitudes may considerably lag surface CH_4 in time and be influenced by the stratosphere. Free troposphere measurements have been used as background references in previous studies of CO_2 (including its isotopic ratios), which also has a large background signal (Ballantyne et al., 2010; Miller et al., 2012). We do not use west coast sites as background reference for all CONUS sites since a large fraction of the air masses we measure are not from the western sector directly (see Figure S2 for average wind pattern). The vertical gradient of CH_4 has been proposed as a more sensitive indicator of surface emissions than horizontal gradients (Bruhwiler et al., 2017). When CH_4 is emitted at the surface, the enhanced CH_4 is mostly retained within the planetary boundary layer (typically below 2.5 km above sea level) for several days, while the free troposphere receives a considerably smaller local influence and mostly represents well-mixed background air (Sweeney et al., 2015). East coast sites that are downwind of CONUS emissions show much larger vertical gradients (39.3 ppb for the average of the NHA and SCA sites; see Table S2) than the west coast inflow site (12.0 ppb at ESP).

We expect to detect trends in vertical gradients if there are increases in surface emissions from locations upwind of a measurement site and no significant change in transport patterns. Our footprint analysis finds that all of the GGGRN sites have similar patterns of surface influences during the first and second halves of the past decade (Figure S4). However, we find no significant trends, meaning the estimated trend is less than1σ uncertainty of the trend, in the CH_4 vertical gradients (ΔCH_4) at most non-ONG sites (Figures 2 and S6). The average trend in ΔCH_4 is -0.21 ± 0.10 ppb/year (-1.00 ± 0.36%/year) for non-ONG sites. For the five ONG sites, the average trend is 1.14 ± 0.30 ppb/year (2.05 ± 0.58%/year). The average trend for

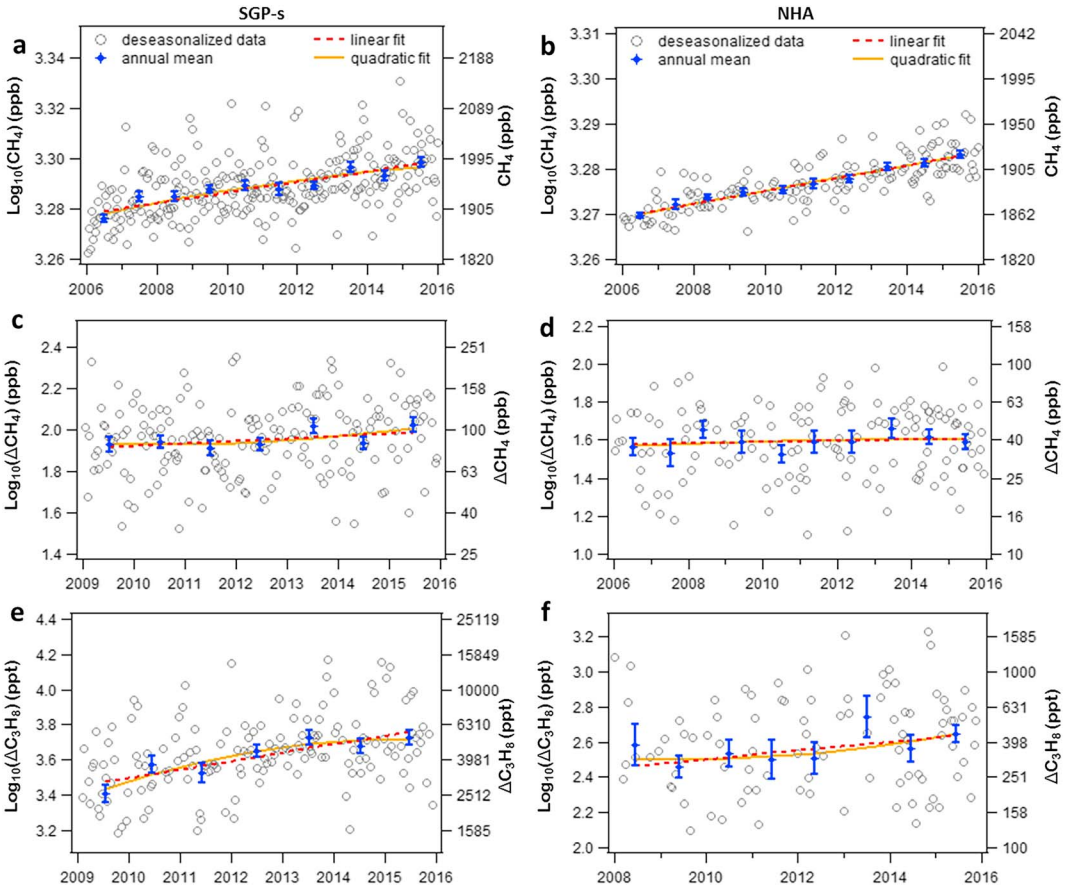

Figure 1. Methane and propane data and trend fits. Left column shows data from Southern Great Plains, Oklahoma (SGP-s, an ONG site), and right column shows data from Worcester, Massachusetts (NHA, an east coast outflow site; see Figure S2 for average wind pattern). (a and b) Deseasonalized data and trend fits to those data. For the aircraft site (NHA), those data are the averages below 2.5 km above sea level. (c and d) CH_4 vertical gradients (ΔCH_4) and trend fits to those data. (e and f) C_3H_8 vertical gradients (ΔC_3H_8) and trend fits to those data. Trend fits are performed to annual means and are weighted by the standard errors of the mean (blue error bars; SI section 2). The left axes are in $\log_{10}$ scale (see SI section 2 for details); labels on the right axes show corresponding values of the ticks on the left axes. Trends are presented in Figures 2 and S6.

east coast sites is -0.12 ± 0.16 ppb/year (-0.10 ± 0.50%/year). Note that trends in ΔCH_4 are contributed by both anthropogenic and natural sources. However, we find strong correlations between ΔCH_4 and ΔC_3H_8 (a tracer for ONG emissions) in winter even for non-ONG sites (Figure S5), which is likely due to the reduction in natural CH_4 emissions during wintertime. Despite the increased wintertime correlation between ΔCH_4 and ΔC_3H_8 and the steeper vertical gradients due to the reduced vertical transport, there is no evidence of an increased trend in ΔCH_4 during winter (Figure S7) as would be expected if there were significant increases in ONG CH_4 emissions.

The GGGRN sites are sensitive to ONG emissions because their footprint areas include major ONG production basins in CONUS (Figure S3). However, we find moderate increases in ΔCH_4 from three out of five ONG sites (DND, SGP-s, and WKT-s). If we use the ONG trends from these three sites to represent the ONG emissions trend in the United States (see SI section 5 for calculation), the average (weighted by upwind ONG CH_4 emissions) annual growth rate would be 3.4 ± 1.4%/year or 0.3 ± 0.1 Tg/year^2 as a long-term average (note that the relative trend in %/year is independent of inventory estimates of emissions). This estimate is about an order of magnitude lower than estimates from several previous studies showing 2.1–4.4 Tg/year^2 increase (Turner et al., 2016, Franco et al., 2016, Hausmann et al., 2016, Helmig et al., 2016; note different but overlapping study periods). Nevertheless, a few studies suggest an underestimate in the magnitude of CH_4 emissions in inventories (e.g., Alvarez et al., 2018; Brandt et al., 2014; Miller et al., 2013); our study does not address the magnitude of emissions but only focuses on the trend in emissions that can be estimated

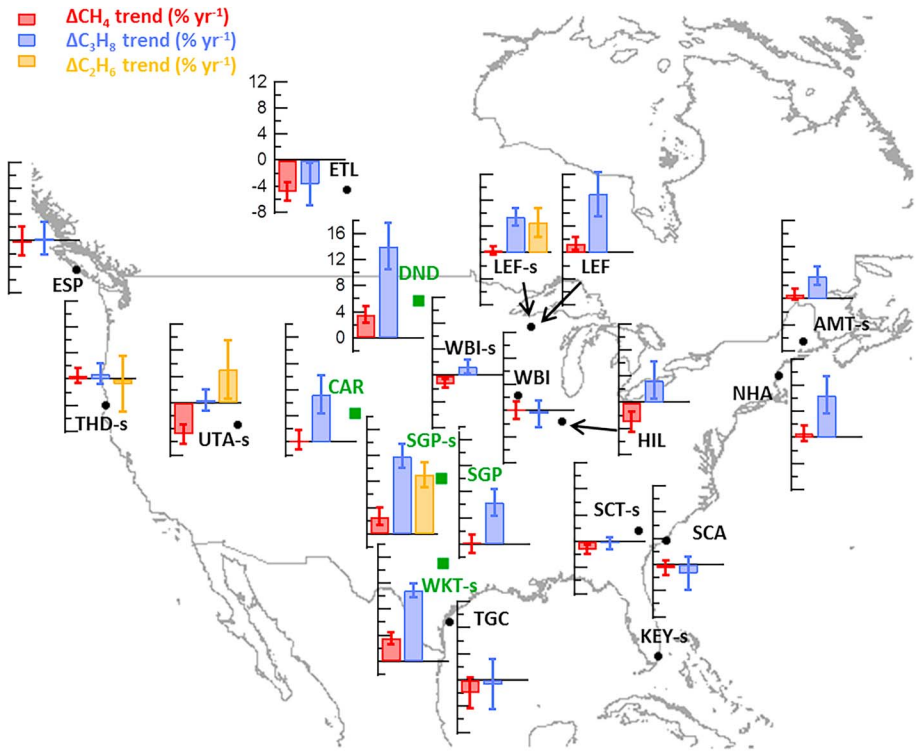

Figure 2. Trends in CH_4, C_3H_8, and C_2H_6 enhancements ('Δ') over North America in recent years (2006-2015 for CH_4 and 2008-2015 for C_2H_6 and C_3H_8 for most sites; see Table S1.). The green squares and black dots show ONG and non-ONG sites, respectively. '-s' following a site code indicates surface site. For all bar charts each tick increment is 2%/year and the horizontal axis crosses at 0%/year (e.g., ETL and DND); '%/year' means increase of Δ relative to previous year; see Table S2 for values, and trends in ppb/year for CH_4 or in ppt/year for C_2H_6 and C_3H_8. The error bars show 1σ uncertainty. For CH_4 and C_3H_8, enhancements are relative to midtroposphere measurements (thus, the trends are for vertical gradients, also see Figure S6). For C_2H_6, enhancements are relative to the Marine Boundary Layer background (SI section 3).

directly from atmospheric observations. This relatively small trend in ONG emissions (3.4 ± 1.4%/year) is challenging for the east coast sites to detect.

How much do CH_4 emissions need to increase to be detected by the GGGRN? Since the relative trend in vertical gradients is equal to the relative trend in total regional emissions (both as %/year changes) considering no significant secular changes in atmospheric transport/mixing (as shown in Figure S4), the uncertainty of the trend in vertical gradients can serve as an indicator for the detectability of the trend in emissions. Note that the variability in midtroposphere background has been accounted for in estimating the trend uncertainty (SI section 3). We find that more than half of the sites have trend uncertainties (1σ) smaller than 1.3%/year (Table S2), which suggests at least half of GGGRN sites can likely detect a relative change of total CH_4 emissions greater than 1.3%/year (averaged over the 10-year period). The detectability thresholds across four east coast sites (NHA, SCA, SCT-s, and AMT-s) range from 0.7 to 1.2 %/year. Our estimated ONG emission trend of 3.4 ± 1.4%/year corresponds to a 0.7 ± 0.3%/year increase in total U.S. emissions assuming that ONG emissions account for 20% of total emissions (United States EPA, 2017, Saunois et al., 2016). Thus, these east coast sites are not sensitive enough to clearly capture the relatively small ONG emissions trend (meaning 0.7 ± 0.3%/year is not significantly higher than detectability thresholds for east coast sites). Increasing the numbers of vertical profiles and sampling sites would help to decrease uncertainty in trends and better monitor changes in ONG emissions. However, if the large trends of ONG emissions proposed by previous studies exist (Franco et al., 2016; Hausmann et al., 2016; Helmig et al., 2016; Turner et al., 2016), which correspond to trends in total CH_4 emissions of 5.2–11.0%/year, the east coast sites are capable of detecting them. Such large trends are not apparent in our measurement data from east coast sites making the suggested large increases in U.S. ONG emissions highly unlikely. Note that our trend and detectability are directly calculated from long-term observations, and influences of temporal coverage are fully

considered during calculations (SI section 3). Thus, they are more definitive than model results (Bruhwiler et al., 2017) that are subject to transport and other errors.

In principle, a significant decrease in agricultural CH_4 emissions (mainly from livestock) could have cancelled the increases in ONG emissions given that both emissions are of similar magnitude (United States EPA, 2017). The footprint regions of two ONG sites (SGP-s and WKT-s) overlap with important cattle production regions. To evaluate the potential impact of a livestock emission trend on estimated ONG trends, we impose an agriculture emission trend (-1.7%/year for 2006-2013; Wolf et al., 2017) in calculating the new ONG trends for these two ONG sites (SI section 5). The new ONG trends are 3.2 ± 1.3%/year and 4.8± 1.0%/year for SGP-s and WKT-s, respectively, which are within the uncertainty ranges of our previous estimates. This is expected because both sites are dominated by ONG emissions and non-ONG emissions account for less than 15% of the CH_4 enhancements (Wolf et al., 2017).

We have looked into the influences of non-ONG emissions from measurements at sites that are further away from major ONG production fields, for example, the Great Lakes region. Measurement sites (LEF, LEF-s, WBI, WBI-s, and HIL) in this region have less than 50% ONG influence according to our footprint and inventory analysis. In the warm months, we find increments of ΔCH_4 without increments of ΔC_3H_8 (see Figure S5a for LEF site), indicating possible influences from non-ONG CH_4 emissions and/or increased C_3H_8 losses from faster reactions with hydroxyl radical under higher temperature. Livestock CH_4 emissions from inventories show hot spots in the Great Lake region (Hristov et al., 2017; Maasakkers et al., 2016). In addition, the Great Lake region is also downwind of major wetlands (Lehner & Doll, 2004). Thus, the Great Lakes sites should be sensitive to livestock and wetland CH_4 emissions. The mean trend of ΔCH_4 in these sites is -0.5%/year. Given the estimated trend detectability of 0.5%/year (estimated using $\sqrt{\sum_1^5 \left(\frac{\sigma_i}{5}\right)^2}$; deseasonalized data from each site are independent due to different sampling times and frequencies), increases in total emissions in the Great Lakes region are highly unlikely. Even though these sites are influenced by ONG emissions in winter judging from the strong correlation between ΔC_3H_8 and ΔCH_4 (Figure S5b), we do not find statistically significant CH_4 trends in winter (Figure S7). Since there are no significant changes in total emissions or ONG emissions in the Great Lakes region, it then implies no significant changes in non-ONG CH_4 emissions in this region in the past decade.

3. Discrepancies Between Trends in ΔC_2H_6 and ΔC_3H_8 and Trends in ΔCH_4

Our study also finds much larger relative trends (in %/year) in C_2H_6 and C_3H_8 enhancements (i.e., ΔC_2H_6 and ΔC_3H_8) than in ΔCH_4; even at ONG sites that ΔCH_4 signals are mostly contributed by ONG activities only (Figure 2). Both C_2H_6 and C_3H_8 are coemitted with CH_4 from most ONG sources, and they have much smaller background values than CH_4 (due to shorter atmospheric lifetimes (Goldstein et al., 1995, Rudolph, 1995) and lower emissions), which make them good tracers for ONG emissions. Much larger relative trends (in %/year) in C_3H_8 vertical gradients (ΔC_3H_8) than in ΔCH_4 are consistently observed at ONG sites (Figure 2). This suggests larger percentage increases in C_3H_8 emission than in CH_4 emission from the upwind regions of the sites. For the five ONG sites, the average trend in ΔC_3H_8 is 10.12 ± 1.09%/year (see Table S2 for trends in ppt/year); for non-ONG sites, the average trend is 1.74 ± 0.64%/year. Long-term records of C_2H_6 are only available at a few CONUS surface sites. For C_2H_6 enhancements (ΔC_2H_6), the trend at SGP-s (an ONG site) is the largest, 6.95 ± 1.28 %/year.

4. Discrepancies Between Observed and Calculated ΔCH_4 Trends Using ΔC_2H_6 or ΔC_3H_8

Strong linear correlations between CH_4 and C_2H_6 enhancements (ΔCH_4 and ΔC_2H_6) have been reported from previous ONG field studies with spatially different enhancement ratios (ERs; Peischl et al., 2015, 2016, Smith et al., 2015, Helmig et al., 2014). These ERs may be representative of relative emission rates at the time of the measurement but have been used to estimate trends in ONG CH_4 emissions over longer periods (Franco et al., 2016; Hausmann et al., 2016; Helmig et al., 2016). In contrast, our study determines CH_4 trends in emissions directly from CH_4 observations, and we find much smaller increases in CH_4 ONG emissions than those studies. To investigate this discrepancy, we compared the observed trends of ΔCH_4 with ΔCH_4 trends estimated using ΔC_2H_6 or ΔC_3H_8 trends and their ERs at SGP and SGP-s (ONG sites). We

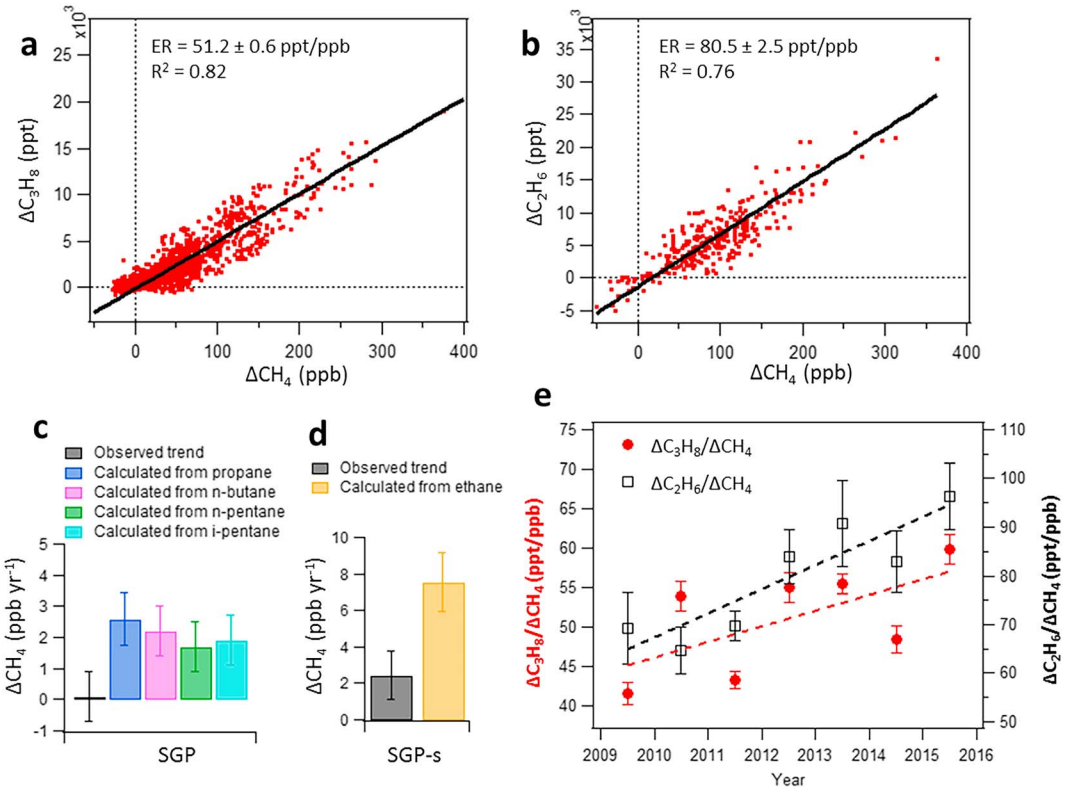

Figure 3. Enhancement ratios (ERs) and discrepancies between observed and calculated ΔCH_4 trends. (a) ER of $\Delta C_3H_8/\Delta CH_4$ from aircraft measurements at SGP during 2009-2015. (b) ER of $\Delta C_2H_6/\Delta CH_4$ from surface flasks measurements at SGP-s during 2009-2015. (c and d) The observed and calculated ΔCH_4 trends using hydrocarbon data and their corresponding ERs (constant ERs from slopes in a and b). ERs in e are the same as in a and b but are derived on yearly basis. The dashed lines are linear fits to the ers; the trend for $\Delta C_3H_8/\Delta CH_4$ is 1.98 ± 1.09 ppt · ppb^{-1} · year^{-1} (red line) and 4.94 ± 1.13 ppt · ppb^{-1} · year^{-1} for $\Delta C_2H_6/\Delta CH_4$ (black line). All error bars shows 1σ uncertainty.

find strong correlations between ΔC_2H_6 and ΔCH_4 at SGP-s, and ΔC_3H_8 and ΔCH_4 at SGP imply that most ΔCH_4 is from ONG emissions and influences from other sources (which do not contribute to ΔC_3H_8 and ΔC_2H_6) are not significant (also note that intercept is close to zero in Figures 3a and 3b). This is consistent with our footprint and inventory analysis.

The linear correlation can be written as

$$\Delta HC = ER \times \Delta CH_4 + \text{intercept} \quad (1)$$

Taking the time derivative of equation (1) gives

$$\frac{d(\Delta HC)}{dt} = ER \times \frac{d(\Delta CH_4)}{dt} + \Delta CH_4 \times \frac{d(ER)}{dt} \quad (2)$$

If ER is assumed constant over time (as done in previous studies (Franco et al., 2016, Hausmann et al., 2016, Helmig et al., 2016)), equation (2) becomes

$$\frac{d(\Delta HC)}{dt} = ER \times \frac{d(\Delta CH_4)}{dt} \quad (3)$$

where ΔHC represents the enhancement of any hydrocarbon compound that is well correlated with ΔCH_4. Equation (3) has been used in other studies to derive ΔCH_4 trends from ONG emissions. However, when we apply equation (3), i.e., using the observed average $\Delta C_3H_8/\Delta CH_4$ (from Figure 3a) and the observed ΔC_3H_8 trend to calculate ΔCH_4 trend ($\frac{d(\Delta CH_4)}{dt}$) at SGP, we derive a ΔCH_4 trend that is much larger than the observed

trend (Figure 3c) because the missing term $\Delta CH_4 \times \frac{d\,(ER)}{dt}$ (due to simplification from equations (2) and (3)) has to be compensated by the derived ΔCH_4 trend. A similar overestimate in calculated ΔCH_4 trend is also found when using the average ER of $\Delta C_2H_6/\Delta CH_4$ (Figure 3d, and for butane and pentanes; Figure 3c). These discrepancies are caused in part from ERs varying over time (see Figure 3e). As an example for SGP-s, the observed ΔC_2H_6 trend ($\frac{d(\Delta HC)}{dt}$) equals 610 ± 130 ppt/year, while $\Delta \mathbf{CH_4} \times \frac{d\,(ER)}{dt}$ Equals 494 ± 113 ppt/year for 2009–2015. Note that multiplying $\frac{d\,(ER)}{dt}$ With $\mathbf{\Delta CH_4}$ amplified the impact of the temporal variations of ER substantially. Thus, the simplified relationship in equation (3) is not valid. If equation (2) is used, the resulting ΔCH_4 trend is 1.44 ± 2.14 ppb/year, which is much closer to the observed 2.30 ± 1.18 ppb/year than using equation (3) (see Figure 3d). However, the large uncertainty in the 1.44 ± 2.14 ppb/year trend makes the trend statistically insignificant ($\sigma > 1.44$ ppb/year). This uncertainty mostly comes from the uncertainty of the observed ΔC_2H_6 trend and the uncertainty of the trend in ER which partially due to the imperfect correlation between ΔC_2H_6 and ΔCH_4. Thus, equation (2) is not an optimized approach to estimate ΔCH_4 trend; instead, directly measurements provide better estimate.

The ONG production data reported by the U.S. Energy Information Agency (U.S. Energy Information Administration) demonstrate drastically different production trends for dry natural gas, C_2H_6 and C_3H_8 in the surrounding regions of SGP, with 36%, 99%, and 132% increases, respectively, in the last decade (Figure S1). The much higher relative increases in C_2H_6 and C_3H_8 than CH_4 productions are qualitatively consistent with our findings about larger increases in ΔC_2H_6 and ΔC_3H_8 than ΔCH_4 (Figure 2) and the increasing trends in $\Delta C_2H_6/\Delta CH_4$ and $\Delta C_3H_8/\Delta CH_4$ (Figure 3e). These suggest that the total CH_4, C_2H_6, and C_3H_8 emissions from ONG activities may have increased at substantially different rates, reflecting the fundamental heterogeneity of ONG activities with respect to these chemicals, and possibly depending on economic shifts in the relative profitability of dry natural gas and other hydrocarbons. Previous short-term studies (Kort et al., 2016; Peischl et al., 2015) have reported large spatial differences in ERs from different ONG production fields, questioning the reliability of using a spatially universal ER to estimate ONG CH_4 emissions for continental scale. Our study based on continuous long-term measurements further demonstrates how long-term trends in ER yield faulty ONG CH_4 trend. The ER is neither spatially uniform nor constant in time. Assuming otherwise is not a reliable approach to infer ONG CH_4 trends.

5. Conclusions

Our analysis of direct mole fraction measurements suggests smaller increases in ONG CH_4 emissions from the United States than those reported by several studies (Franco et al., 2016; Hausmann et al., 2016; Helmig et al., 2016; Turner et al., 2016). Although C_2H_6 and C_3H_8 are appropriate indicative tracers for ONG emissions, ONG CH_4 trends cannot be accurately estimated from C_2H_6 and C_3H_8. Thus, any conclusion of a large fossil CH_4 increase in the past decade from studies that have used the constant ER assumption is unreliable. By comparing the ΔCH_4 trend from inflow and outflow sites of CONUS and considering the detectabilities of emission changes at these sites, we find no evidence to support a large increase in total U.S. CH_4 emissions over the past decade, although we do find clear evidence of a modest increase in ONG CH_4 emissions at three sites. By comparing the ΔCH_4 trend with trends in ΔC_2H_6 and ΔC_3H_8 at ONG sites, we also find that the increases in ONG C_2H_6 and C_3H_8 emissions are substantially larger on a relative basis than increases in ONG CH_4 emissions.

Acknowledgments
We thank Doug Guenther, Jack Higgs, Eric Moglia, Don Neff, and Sonja Wolter for their contributions to data collection; Andrew Crotwell for air sample analysis; Anna Karion for contributions to the aircraft sampling; Carolina Siso for conducting propane analysis; and Brad Hall for providing standard scales for propane and ethane. We thank NOAA Climate Program Office for supporting this study. Observations collected at the Southern Great Plains site were supported by the Office of Biological and Environmental Research of the US Department of Energy under contract DE-AC02-05CH11231 as part of the Atmospheric Radiation Measurement Program (ARM) and Terrestrial Ecosystem Science (TES) Program. Methane mole fraction data from aircraft measurements and surface flasks are provided by NOAA/OAR/ESRL GMD, publically available at https://www.esrl.noaa.gov/gmd/ccgg/obspack/data.php?Id=obspack_multi-species_1_ccggaircraftflask_v1.0_2018-02-08. Https://www.esrl.noaa.gov/gmd/ccgg/obspack/data.php?Id=obspack_multi-species_1_ccggsurfaceflask_v1.0_2018-02-08. Aircraft and tall tower measured propane, butane, and pentanes data used in this research are available at https://doi.org/10.15138/G3W92R. Surface ethane and propane data (including KEY-s, THD-s, UTA-s, SGP-s, and MLO-s sites in this study) are publically available at https://www.esrl.noaa.gov/gmd/dv/data/. NCEP Reanalysis data provided by the NOAA/OAR/ESRL PSD, Boulder, Colorado, USA, from their web site at https://www.esrl.noaa.gov/psd/.

References

Alvarez, R. A., Zavala-Araiza, D., Lyon, D. R., Allen, D. T., Barkley, A. R., Brandt, A. R., et al. (2018). Assessment of methane emissions from the U.S. oil and gas supply chain. *Science*, *361*, 186–188. https://doi.org/10.1126/science.aar7204

Andrews, A. E., Kofler, J. D., Trudeau, M. E., Williams, J. C., Neff, D. H., Masarie, K. A., et al. (2014). CO_2, CO, and CH_4 measurements from tall towers in the NOAA Earth System Research Laboratory's Global Greenhouse Gas Reference Network: Instrumentation, uncertainty analysis, and recommendations for future high-accuracy greenhouse gas monitoring efforts. *Atmospheric Measurement Techniques*, *7*(2), 647–687. https://doi.org/10.5194/amt-7-647-2014

Ballantyne, A. P., Miller, J. B., & Tans, P. P. (2010). Apparent seasonal cycle in isotopic discrimination of carbon in the atmosphere and biosphere due to vapor pressure deficit. *Global Biogeochemical Cycles*, *24*, GB3018. https://doi.org/10.1029/2009GB003623

Bousquet, P., Ciais, P., Miller, J. B., Dlugokencky, E. J., Hauglustaine, D. A., Prigent, C., et al. (2006). Contribution of anthropogenic and natural sources to atmospheric methane variability. *Nature*, *443*(7110), 439–443. https://doi.org/10.1038/nature05132

Brandt, A. R., Heath, G. A., Kort, E. A., O'Sullivan, F., Petron, G., Jordaan, S. M., et al. (2014). Methane leaks from North American Natural Gas Systems. *Science*, *343*(6172), 733–735. https://doi.org/10.1126/science.1247045

Bruhwiler, L. M., Basu, S., Bergamaschi, P., Bousquet, P., Dlugokencky, E., Houweling, S., et al. (2017). US CH_4 emissions from oil and gas production: Have recent large increases been detected? *Journal of Geophysical Research: Atmospheres*, *122*, 4070–4083. https://doi.org/10.1002/2016JD026157

Butler, J. H., & Montzka, S. A. (2017). THE NOAA Annual Greenhouse Gas Index (AGGI). https://www.esrl.noaa.gov/gmd/aggi/aggi.html

Dlugokencky, E. (2018). Trends in atmospheric methane. *NOAA/ESRL*, https://www.esrl.noaa.gov/gmd/ccgg/trends_ch4/

Dlugokencky, E. J., Bruhwiler, L., White, J. W. C., Emmons, L. K., Novelli, P. C., Montzka, S. A., et al. (2009). Observational constraints on recent increases in the atmospheric CH4 burden. *Geophysical Research Letters*, *36*, L18803. https://doi.org/10.1029/2009GL039780

Dlugokencky, E. J., Houweling, S., Bruhwiler, L., Masarie, K. A., Lang, P. M., Miller, J. B., & Tans, P. P. (2003). Atmospheric methane levels off: Temporary pause or a new steady-state? *Geophysical Research Letters*, *30*(19), 1992. https://doi.org/10.1029/2003GL018126

Dlugokency, E. J., Lang, P. M., Crotwell, A. M., Masarie, K. A., Crotwell, M. J., & Tans, P. P. (2015). Atmospheric methane dry air mole fractions from the NOAA ESRL Carbon Cycle Cooperative Global Air Sampling Network. Data Path: ftp://aftp.cmdl.noaa.gov/data/trace_gases/ch4/flask/surface/

Franco, B., Mahieu, E., Emmons, L. K., Tzompa-Sosa, Z. A., Fischer, E. V., Sudo, K., et al. (2016). Evaluating ethane and methane emissions associated with the development of oil and natural gas extraction in North America. *Environmental Research Letters*, *11*(4), 11. https://doi.org/10.1088/1748-9326/11/4/044010

Goldstein, A. H., Wofsy, S. C., & Spivakovsky, C. M. (1995). Seasonal-variations of nonmethane hydrocarbons in rural New England—Constraints on OH concentrations in northern midlatitudes. *Journal of Geophysical Research*, *100*(D10), 21,023–21,033. https://doi.org/10.1029/95JD02034

Hausmann, P., Sussmann, R., & Smale, D. (2016). Contribution of oil and natural gas production to renewed increase in atmospheric methane (2007-2014): Top-down estimate from ethane and methane column observations. *Atmospheric Chemistry and Physics*, *16*(5), 3227–3244. https://doi.org/10.5194/acp-16-3227-2016

Helmig, D., Rossabi, S., Hueber, J., Tans, P., Montzka, S. A., Masarie, K., et al. (2016). Reversal of global atmospheric ethane and propane trends largely due to US oil and natural gas production. *Nature Geoscience*, *9*(7), 490–495. https://doi.org/10.1038/ngeo2721

Helmig, D., Thompson, C. R., Evans, J., Boylan, P., Hueber, J., & Park, J. H. (2014). Highly elevated atmospheric levels of volatile organic compounds in the Uintah Basin, Utah. *Environmental Science & Technology*, *48*(9), 4707–4715. https://doi.org/10.1021/es405046r

Hristov, A. N., Harper, M., Meinen, R., Day, R., Lopes, J., Ott, T., et al. (2017). Discrepancies and uncertainties in bottom-up gridded inventories of livestock methane emissions for the contiguous United States. *Environmental Science & Technology*, *51*(23), 13,668–13,677. https://doi.org/10.1021/acs.est.7b03332

Kort, E. A., Smith, M. L., Murray, L. T., Gvakharia, A., Brandt, A. R., Peischl, J., et al. (2016). Fugitive emissions from the Bakken shale illustrate role of shale production in global ethane shift. *Geophysical Research Letters*, *43*, 4617–4623. https://doi.org/10.1002/2016GL068703

Lehner, B., & Doll, P. (2004). Development and validation of a global database of lakes, reservoirs and wetlands. *Journal of Hydrology*, *296*(1-4), 1–22. https://doi.org/10.1016/j.jhydrol.2004.03.028

Maasakkers, J. D., Jacob, D. J., Sulprizio, M. P., Turner, A. J., Weitz, M., Wirth, T., et al. (2016). Gridded National Inventory of US Methane Emissions. *Environmental Science & Technology*, *50*(23), 13,123–13,133. https://doi.org/10.1021/acs.est.6b02878

Miller, J. B., Lehman, S. J., Montzka, S. A., Sweeney, C., Miller, B. R., Karion, A., et al. (2012). Linking emissions of fossil fuel CO_2 and other anthropogenic trace gases using atmospheric (CO2)-C-14. *Journal of Geophysical Research*, *117*, D08302. https://doi.org/10.1029/2011JD017048

Miller, S. M., Wofsy, S. C., Michalak, A. M., Kort, E. A., Andrews, A. E., Biraud, S. C., et al. (2013). Anthropogenic emissions of methane in the United States. *Proceedings of the National Academy of Sciences of the United States of America*, *110*(50), 20,018–20,022. https://doi.org/10.1073/pnas.1314392110

Nisbet, E. G., Dlugokencky, E. J., Manning, M. R., Lowry, D., Fisher, R. E., France, J. L., et al. (2016). Rising atmospheric methane: 2007-2014 growth and isotopic shift. *Global Biogeochemical Cycles*, *30*, 1356–1370. https://doi.org/10.1002/2016GB005406

Peischl, J., Karion, A., Sweeney, C., Kort, E. A., Smith, M. L., Brandt, A. R., et al. (2016). Quantifying atmospheric methane emissions from oil and natural gas production in the Bakken shale region of North Dakota. *Journal of Geophysical Research: Atmospheres*, *121*, 6101–6111. https://doi.org/10.1002/2015JD024631

Peischl, J., Ryerson, T. B., Aikin, K. C., de Gouw, J. A., Gilman, J. B., Holloway, J. S., et al. (2015). Quantifying atmospheric methane emissions from the Haynesville, Fayetteville, and northeastern Marcellus shale gas production regions. *Journal of Geophysical Research: Atmospheres*, *120*, 2119–2139. https://doi.org/10.1002/2014JD022697

Rudolph, J. (1995). The tropospheric distribution and budget of ethane. *Journal of Geophysical Research*, *100*(D6), 11,369–11,381. https://doi.org/10.1029/95JD00693

Saunois, M., Bousquet, P., Poulter, B., Peregon, A., Ciais, P., Canadell, J. G., et al. (2016). The global methane budget 2000-2012. *Earth System Science Data*, *8*(2), 697–751. https://doi.org/10.5194/essd-8-697-2016

Schaefer, H., Fletcher, S. E. M., Veidt, C., Lassey, K. R., Brailsford, G. W., Bromley, T. M., et al. (2016). A 21st-century shift from fossil-fuel to biogenic methane emissions indicated by (CH4)-C-13. *Science*, *352*(6281), 80–84. https://doi.org/10.1126/science.aad2705

Schwietzke, S., Sherwood, O. A., Ruhwiler, L., Miller, J. B., Etiope, G., Dlugokencky, E. J., et al. (2016). Upward revision of global fossil fuel methane emissions based on isotope database. *Nature*, *538*(7623), 88–91. https://doi.org/10.1038/nature19797

Smith, M. L., Kort, E. A., Karion, A., Sweeney, C., Herndon, S. C., & Yacovitch, T. I. (2015). Airborne ethane observations in the Barnett Shale: Quantification of ethane flux and attribution of methane emissions. *Environmental Science & Technology*, *49*(13), 8158–8166. https://doi.org/10.1021/acs.est.5b00219

Sweeney, C., Karion, A., Wolter, S., Newberger, T., Guenther, D., Higgs, J. A., et al. (2015). Seasonal climatology of CO_2 across North America from aircraft measurements in the NOAA/ESRL Global Greenhouse Gas Reference Network. *Journal of Geophysical Research: Atmospheres*, *120*, 5155–5190. https://doi.org/10.1002/2014JD022591

Turner, A. J., Jacob, D. J., Benmergui, J., Wofsy, S. C., Maasakkers, J. D., Butz, A., et al. (2016). A large increase in US methane emissions over the past decade inferred from satellite data and surface observations. *Geophysical Research Letters*, *43*, 2218–2224. https://doi.org/10.1002/2016GL067987

United States Energy Information Administration (2016). Hydraulically fractured wells provide two-thirds of U.S. natural gas production. https://www.eia.gov/todayinenergy/detail.php?Id=26112

United States Environmental Protection Agency (2017). Inventory of U.S. greenhouse gas emissions and sink. 2. Trends in greenhouse gas emissions. https://www.epa.gov/sites/production/files/2017-02/documents/2017_chapter_2_trends_in_greenhouse_gas_emissions.pdf

Wolf, J., Asrar, G. R., & West, T. O. (2017). Revised methane emissions factors and spatially distributed annual carbon fluxes for global livestock. *Carbon Balance and Management*, *12*(1), 16. https://doi.org/10.1186/s13021-017-0084-y

References From the Supporting Information

Biraud, S. C., Torn, M. S., Smith, J. R., Sweeney, C., Riley, W. J., & Tans, P. P. (2013). A multi-year record of airborne CO_2 observations in the US Southern Great Plains. *Atmospheric Measurement Techniques*, *6*(3), 751–763. https://doi.org/10.5194/amt-6-751-2013

Diaconis, P., & Efron, B. (1983). Computer-intensive methods in statistics. *Scientific American*, *248*(5), 116–130.

Dlugokencky, E. J., Myers, R. C., Lang, P. M., Masarie, K. A., Crotwell, A. M., Thoning, K. W., et al. (2005). Conversion of NOAA atmospheric dry air CH4 mole fractions to a gravimetrically prepared standard scale. *Journal of Geophysical Research*, *110*, D18306. https://doi.org/10.1029/2005JD006035

Kalnay, E., Kanamitsu, M., Kistler, R., Collins, W., Deaven, D., Gandin, L., et al. (1996). The NCEP/NCAR 40-year reanalysis project. *Bulletin of The American Meteorological Society*, *77*(3), 437–471.

Lin, J. C., Gerbig, C., Wofsy, S. C., Andrews, A. E., Daube, B. C., Davis, K. J., & Grainger, C. A. (2003). A near-field tool for simulating the upstream influence of atmospheric observations: The Stochastic Time-Inverted Lagrangian Transport (STILT) model. *Journal of Geophysical Research*, *108*(D16), 4493. https://doi.org/10.1029/2002JD003161

Miller, S. M., Commane, R., Melton, J. R., Andrews, A. E., Benmergui, J., Dlugokencky, E. J., et al. (2016). Evaluation of wetland methane emissions across North America using atmospheric data and inverse modeling. *Biogeosciences*, *13*(4), 1329–1339. https://doi.org/10.5194/bg-13-1329-2016

Montzka, S. A., Calvert, P., Hall, B. D., Elkins, J. W., Conway, T. J., Tans, P. P., & Sweeney, C. (2007). On the global distribution, seasonality, and budget of atmospheric carbonyl sulfide (COS) and some similarities to CO2. *Journal of Geophysical Research*, *112*, D09302. https://doi.org/10.1029/2006JD007665

Montzka, S. A., Myers, R. C., Butler, J. H., Elkins, J. W., & Cummings, S. O. (1993). Global tropospheric distribution and calibration scale of HCFC-22. *Geophysical Research Letters*, *20*(8), 703–706. https://doi.org/10.1029/93GL00753

Nehrkorn, T., Eluszkiewicz, J., Wofsy, S. C., Lin, J. C., Gerbig, C., Longo, M., & Freitas, S. (2010). Coupled weather research and forecasting-stochastic time-inverted Lagrangian transport (WRF-STILT) model. *Meteorology and Atmospheric Physics*, *107*(1-2), 51–64. https://doi.org/10.1007/s00703-010-0068-x

Pollmann, J., Helmig, D., Hueber, J., Plass-Dulmer, C. A., & Tans, P. (2008). Sampling, storage, and analysis of C-2-C-7 non-methane hydrocarbons from the US National Oceanic and Atmospheric Administration Cooperative Air Sampling Network glass flasks. *Journal of Chromatography. A*, *1188*(2), 75–87. https://doi.org/10.1016/j.chroma.2008.02.059

Pollmann, J., Helmig, D., Hueber, J., Tanner, D., & Tans, P. P. (2006). Evaluation of solid adsorbent materials for cryogen-free trapping—Gas chromatographic analysis of atmospheric C2-C6 non-methane hydrocarbons. *Journal of Chromatography. A*, *1134*(1-2), 1–15. https://doi.org/10.1016/j.chroma.2006.08.050

Thoning, K. W., Tans, P. P., & Komhyr, W. D. (1989). Atmospheric carbon-dioxide at Mauna Loa Observatory.2. Analysis of the NOAA GMCC data, 1974-1985. *Journal of Geophysical Research*, *94*(D6), 8549–8565. https://doi.org/10.1029/JD094iD06p08549

United States Energy Information Administration Natural Gas Production (2018). https://www.eia.gov/naturalgas/data.php#production.

Werner, C., Davis, K., Bakwin, P., Yi, C. X., Hurst, D., & Lock, L. (2003). Regional-scale measurements of CH4 exchange from a tall tower over a mixed temperate/boreal lowland and wetland forest. *Global Change Biology*, *9*(9), 1251–1261. https://doi.org/10.1046/j.1365-2486.2003.00670.x